High LUMO energy level $C_{60}(OCH_3)_4$ derivatives: Electronic acceptors for photovoltaic cells with higher open-circuit voltage

Lin-Long Deng [a,b], Su-Lan Xie [a], Chao Yuan [a], Rong-Fu Liu [a], Juan Feng [a], Li-Chao Sun [a], Xin Lu [a], Su-Yuan Xie [a,*], Rong-Bin Huang [a], Lan-Sun Zheng [a]

[a] State Key Laboratory for Physical Chemistry of Solid Surfaces and Department of Chemistry, College of Chemistry and Chemical Engineering, Xiamen University, Xiamen 361005, China
[b] Pen-Tung Sah Institute of Micro-Nano Science and Technology, Xiamen University, Xiamen 361005, China

ARTICLE INFO

ABSTRACT

Two regioselective $C_{60}(OCH_3)_4$ derivatives, $C_{60}(OCH_3)_4$-PCBM (a methanofullerene derivative of $C_{60}(OCH_3)_4$, PCBM=[6,6]-phenyl-C_{61}-butyric acid methyl ester) and $C_{60}(OCH_3)_4$-APCBM (an aziridinofullerene derivative of $C_{60}(OCH_3)_4$) were synthesized from $C_{60}Cl_6$ and used as acceptor for polymer solar cells. Revealed by cyclic voltammetry, the LUMO energy levels of $C_{60}(OCH_3)_4$-APCBM and $C_{60}(OCH_3)_4$-PCBM are 0.2 and 0.3 eV higher than that of PCBM, respectively. For the polymer photovoltaic cells with fullerene (PCBM, $C_{60}(OCH_3)_4$-APCBM or $C_{60}(OCH_3)_4$-PCBM) acceptor in combination with poly(3-hexylthiophene) (P3HT) donor, the open-circuit voltage is increased from 0.58 V (for PCBM) to 0.63 V (for $C_{60}(OCH_3)_4$-APCBM) and 0.72 V (for $C_{60}(OCH_3)_4$-PCBM). The higher open-circuit voltages are reasonably attributed to the higher LUMO levels of the $C_{60}(OCH_3)_4$ derivatives because of four electron-donating methoxy groups attached. The photovoltaic performance of $C_{60}(OCH_3)_4$-PCBM-based device is higher than that involving $C_{60}(OCH_3)_4$-APCBM, largely due to the structural change-ability of $C_{60}(OCH_3)_4$-APCBM resulting from the rotatable N–C bond bridge therein. This work demonstrates that fullerene derivatives with higher LUMO level can be functionalized from multi-addition of electron-donating groups, and exemplifies that photovoltaic performances of fullerene-based solar cells are sensitive even to trivial bridge between functional group and fullerene core.

© 2012 Elsevier B.V. All rights reserved.

1. Introduction

Polymer solar cells (PSCs) have attracted much attention due to their advantages such as flexibility and lightweight [1–7]. Hetero-junction polymer photovoltaic cell is currently the most efficient PSC featuring with an active layer consisting of a blend of a conjugated polymer electron donor and an electron acceptor, in which fullerene derivative is the most commonly used electron acceptor superior to those made of polymers [8] or small molecules [9,10]. [6,6]-Phenyl-C_{61}-butyric acid methyl ester (PCBM) and its C_{70} cousin ([6,6]-phenyl-C_{71}-butyric acid methyl ester) are still the most widely used electron acceptors to date [11], largely due to their good solubility, high electron affinity, and high electron mobility. However, the power conversion efficiency (PCE) of the PSCs based on PCBM is limited, to some extent, by the low-lying LUMO energy level of PCBM. Because the open-circuit voltage (V_{oc}) of PSCs is proportional to the energy difference between HOMO of the donor and LUMO of the acceptor [12–16], the relatively lower

LUMO energy level of PCBM in principle leads to lower V_{oc} and, in turn, lower PCE of the PCBM-based photovoltaic device.

Either lowing the HOMO level of the polymer donor or raising the LUMO level of the fullerene acceptor is possible for improving the V_{oc} of PSCs. Although extensive efforts have been paid to developing new donor-acceptor type low bandgap copolymers with low-lying HOMO levels [17–24], modulating the HOMO levels of the polymers remains challenging. The LUMO level of fullerene derivative can be adjusted by chemical modification, especially adding electron donating groups to the fullerene core [12,25–28]. Recent studies demonstrate that modifying fullerene derivative from mono-addition to multi-addition is one of efficient ways to increase the LUMO level of fullerene electron acceptor [29–47]. For example, indene C_{60} bis-adduct (ICBA) has a LUMO level ~0.2 eV higher than that of mono-adduct derivative (ICMA) [32]. Bis-adduct of PCBM (bisPCBM) shows LUMO of ~0.1 eV higher than that of PCBM itself, whereas tri-adduct of PCBM has a LUMO energy level further higher than bisPCBM [30]. Currently available reactions for synthesis of fullerene multi-addition derivatives, however, usually result in a mix of multi-adduct species [29–47]. Such a mixture of electronic acceptors is unfavorable for ordered assembly and electron transfer [48,49],

* Corresponding author.
E-mail address: syxie@xmu.edu.cn (S.-Y. Xie).

and thus limits the otherwise improvable PCE in the photovoltaic cells involved [50]. Effort to isolate individual multi-adduct of fullerene (C_{60} or C_{70}) from the mixed products and sequentially use as electron acceptor in PSCs, however, is fruitless to date. As a result, synthesis of structurally well-defined multi-adduct of fullerene with high-lying LUMO energy level is highly desired.

Here we show a rational synthesis of fullerene multi-adduct with well-defined structure, i.e., $C_{60}(OCH_3)_4$-PCBM (a methano-fullerene derivative of $C_{60}(OCH_3)_4$) and $C_{60}(OCH_3)_4$-APCBM (an aziridinofullerene derivative of $C_{60}(OCH_3)_4$). The subtle structural difference between $C_{60}(OCH_3)_4$-PCBM and $C_{60}(OCH_3)_4$-APCBM facilitates to investigate the relationship between molecular structure and photovoltaic performance. Revealed by cyclic voltammetry, the LUMO energy levels of $C_{60}(OCH_3)_4$-PCBM and $C_{60}(OCH_3)_4$-APCBM are higher than that of PCBM. Blended with poly(3-hexylthiophene) (P3HT), resultantly, $C_{60}(OCH_3)_4$-PCBM and $C_{60}(OCH_3)_4$-APCBM exhibit enhanced V_{oc} in the corresponding photovoltaic devices.

2. Experimental section

2.1. Materials

C_{60} was purchased from Puyang Yongxin Fullerene Co., Ltd. Chlorobenzene and o-dichlorobenzene (o-DCB) were obtained from Alfa-Aesar Company. P3HT was purchased from FEM Technology Co., Inc. and used as received. Other reagents and chemicals were commercially available.

2.2. Measurements

^{1}H NMR and ^{13}C NMR spectra were measured on a Bruker Biospin Advance III 500 MHz spectrometer. Chemical shifts were reported in ppm relative to the singlet of residual $CHCl_3$ at 7.26 for ^{1}H NMR and $CDCl_3$ at 77 ppm for ^{13}C NMR, respectively. The NMR spectra were measured in $CDCl_3$ at room temperature unless noted otherwise. Mass spectra were recorded on a Bruker Esquire HCT mass spectrometer with an atmospheric pressure chemical ionization (APCI) ion source in the negative ion mode. The dry gas temperature was set at 250° C, and the APCI temperature was set at 300° C. Elemental analyses were measured with a Vario EL III CHNOS Elemental Analyzer. UV–vis absorption spectra were obtained on a Varian Cary 5000 UV–vis–NIR spectrophotometer. Cyclic voltammetry was conducted on a CHI-660C electrochemical workstation with Pt disk, Pt wire, and Ag/Ag^+ electrode (0.01 M $AgNO_3$, 0.09 M tetrabutylammonium hexafluorophosphate (Bu_4NPF_6) in acetonitrile) as working electrode, counter electrode, and reference electrode, respectively, in a 0.1 mol/L Bu_4NPF_6 o-dichlorobenzene/acetonitrile (5:1) solution. Atomic force microscopy (AFM) was performed on a Multimode Nanoscope controller IIIa (Veeco Inc.) operated in tapping mode. High performance liquid chromatography (HPLC) analysis was conducted on a Shimadzu liquid chromatography modular system consisting of two LC-20AT pumps, an UV Shimadzu SPD-20 A diode array UV detector, and a CBM-20 A system controller.

2.3. Synthesis of $C_{60}(OCH_3)_4$ derivatives

2.3.1. $C_{60}(OCH_3)_4$

The synthetic route for $C_{60}(OCH_3)_4$ is shown in Scheme 1. $C_{60}Cl_6$ was prepared by chlorinating C_{60} with ICl as described previously by Birkett et al. [51] and was used without further purification. To a solution of $C_{60}Cl_6$ (500 mg, 0.536 mmol) in chlorobenzene (200 mL) was added DMSO (10 mL), and the mixture was stirred under continuous bubbling of O_2 for 5 min. To the solution was then added methanol (10 mL), and was stirred under air at 85 °C for 10 h. The reaction mixture was concentrated in vacuo. The crude product was first purified by silica gel column chromatography using petroleum ether/toluene (3/7, v/v) as eluents to remove most of byproducts. Further purification by semi-preparative HPLC using a Cosmosil 5PBB column (5 μm, 10 mm I.D. × 250 mm) with an eluent of toluene afforded 136 mg of red powder in 30% yield. ^{1}H NMR (500 MHz, $CDCl_3$) δ: 4.03 (s, 6 H), 3.94 (s, 6 H); ^{13}C NMR (125 MHz, $CDCl_3$) δ: 150.80, 149.90, 149.69, 149.53, 147.74, 147.44, 147.22, 147.11, 147.06, 146.99, 146.85, 146.70, 146.38, 146.31, 145.23, 144.81, 144.48, 144.41, 143.73, 143.60, 143.23, 143.06, 142.33, 140.67, 82.51, 78.19, 56.70, 55.80; APCI-MS: $M^- = 844.3$ m/z (calcd. 844.8); elemental analysis calc. for $C_{64}H_{12}O_4$: C, 90.99%; H, 1.43%; found: C, 90.27%; H, 1.39%.

2.3.2. $C_{60}(OCH_3)_4$-PCBM

Methyl-4-benzoylbutyrate p-tosylhydrazone (200 mg, 0.534 mmol) was dissolved in dry pyridine (10 mL) in a dried three-necked flask equipped with N_2 inlet, a thermometer and a magnetic stirring bar. Then, CH_3ONa (30 mg, 0.555 mmol) was added, and the mixture was stirred for 15 min. A solution of 200 mg (0.24 mmol) of $C_{60}(OCH_3)_4$ in 180 mL chlorobenzene was added, and the reaction mixture was stirred at 55° C for 5 h. The reaction mixture was concentrated in vacuo, and then was purified by silica gel column chromatography using toluene as eluent. Further purification by semi-preparative HPLC using a Cosmosil 5PYE column (5 μm, 10 mm I.D. × 250 mm) with an eluent of toluene afforded 90 mg red powder in 37% yield. ^{1}H NMR (500 MHz, $CDCl_3$) δ: 7.69 (d, J=8 Hz, 1 H), 7.54 (m, 1 H), 7.46 (m, 1 H), 7.38 (m, 2 H), 4.06 (s, 3 H), 3.97 (s, 3 H), 3.96 (s, 3 H), 3.64 (s, 3 H), 3.21 (s, 3 H), 3.08 (m, 1 H), 2.92 (m, 1 H), 2.43 (m, 1 H), 2.36 (m, 1 H), 1.94 (m, 1 H), 1.85 (m, 1 H); ^{13}C NMR (125 MHz, $CDCl_3$) δ: 173.59, 149.51, 149.46, 149.25, 149.09, 148.47, 148.42, 147.90, 147.86, 147.81, 147.75, 147.57, 147.54, 147.34, 147.25, 147.22, 147.09, 146.93, 146.90, 146.89, 146.46, 145.27, 144.82, 143.84, 143.78, 143.70, 143.65, 142.01, 139.58, 131.91, 130.09, 128.58, 127.96, 127.59, 82.30, 81.67, 69.97, 66.03, 59.36, 55.56, 55.43, 55.34, 55.05, 51.56, 37.87, 33.76, 23.14; APCI-MS: $M^- = 1034.2$ m/z (calcd. 1035.0); elemental analysis calc. for $C_{76}H_{26}O_6$: C, 88.19%; H, 2.53%; found: C, 86.93%; H, 2.51%.

2.3.3. $C_{60}(OCH_3)_4$-APCBM

A mixture of 5-azido-5-phenylpentanoate (70 mg, 0.30 mmol), $C_{60}(OCH_3)_4$ (200 mg, 0.24 mmol) and chlorobenzene (180 mL) was placed in a round-bottom flask under N_2 and stirred at room temperature for 15 min. The homogeneous mixture was stirred at 100° C under N_2 for 36 h. The solution was heated to 110° C and was stirred for 6 h, followed by heated to 120° C and stirred for 12 h. After cooling to room temperature, the reaction mixture was concentrated under reduced pressure. The crude product was purified by semi-preparative HPLC using a Cosmosil 5PBB column (5 μm, 10 mm I.D. × 250 mm) with an eluent of toluene to afford 108 mg red powder in 43% yield. ^{1}H NMR (500 MHz, $CDCl_3$) δ: 7.68 (broad, 1 H), 7.54 (broad, 1 H), 7.49 (broad, 1 H), 7.35 (broad, 2 H), 5.20 (t, J=8 Hz, 1 H), 3.57–4.07 (m, 15 H), 2.46 (broad, 1 H), 2.35 (broad, 1 H), 2.17 (broad, 2 H), 1.81 (m, 2 H), 1.63 (broad, 1 H); ^{13}C NMR (125 MHz, $CDCl_3$) δ: 173.61, 152.11, 151.56, 150.99, 150.30, 149.45, 147.79, 147.69, 147.29, 147.02, 146.84, 146.44, 145.88, 145.17, 144.73, 144.67, 144.47, 143.65, 142.96, 142.00, 141.28, 140.51, 128.58, 127.73, 127.52, 126.99, 82.45, 78.08, 72.52, 67.24, 66.15, 65.51, 65.35, 64.88, 57.32, 56.77, 55.50, 51.48, 38.64, 37.26, 34.15, 29.65, 21.11; APCI-MS: $M^- = 1049.3$ m/z (calcd. 1050.0); elemental analysis calc. for $C_{76}H_{27}NO_6$: C, 86.93%; H, 2.59%; N, 1.33%; found: C, 86.14%; H, 2.53 %; N, 1.32%.

Scheme 1. Synthesis of $C_{60}(OCH_3)_4$ derivatives .
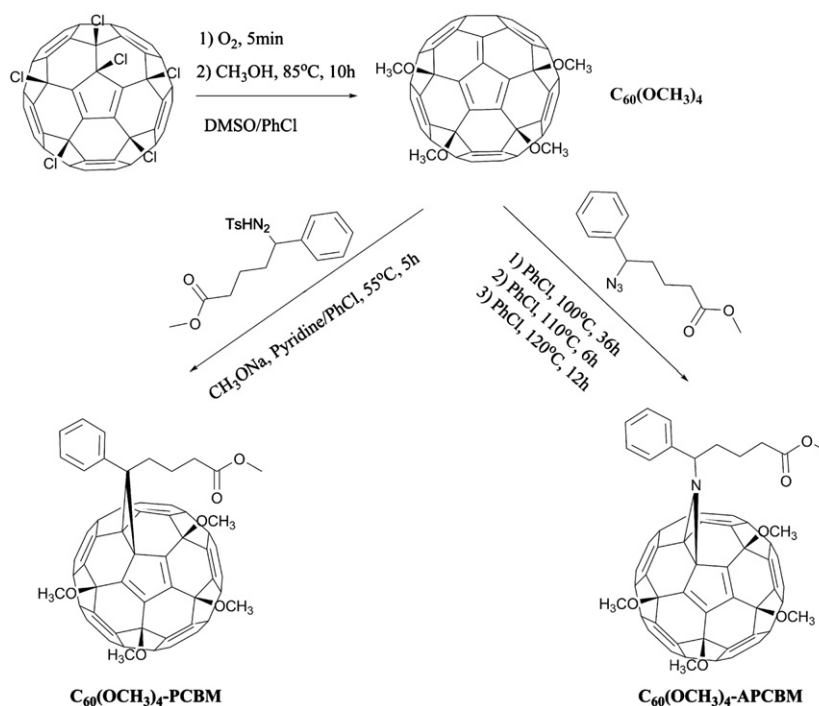
2.4. Fabrication and characterization of PSCs

PSCs with the configuration of ITO/PEDOT:PSS/P3HT:fullerene/Ca/Al were fabricated. Patterned ITO glass substrate ($10 \, \Omega/\square$, purchased from CSG Holding Co., Ltd. China) was cleaned by sequential ultrasonic treatment in detergent, deionized water, acetone, and isopropyl alcohol, and then dried overnight in an oven at $80°$ C. The ITO glass was treated in a UV ozone chamber for 10 min prior to spin-coating a thin (~ 30 nm) poly(ethylene-dioxythiophene): poly(styrenesulfonic acid) (PEDOT:PSS) (Baytron P VP AI 4083) layer at 4000 rpm for 30 s. The substrate was baked at $140°$ C in air for 10 min, and then moved into a glove box for spin-coating the photoactive layer. The blend solution of P3HT and fullerene derivatives in o-DCB (1:1 w/w, 34 mg/mL) was spin-coated on the top of PEDOT:PSS layer at 600 rpm for 60 s. The wet blend films were then kept into a glass Petri dish overnight to undergo solvent annealing process, forming a photoactive layer with a thickness of ~ 180 nm. Finally, a cathode consisted of ~ 20 nm Ca and ~ 100 nm Al was deposited by thermal evaporation under a vacuum of $\sim 2 \times 10^{-4}$ Pa through a shadow mask. The area of device is $\sim 0.10 \, cm^2$ for each solar cell discussed in this work. All the devices were encapsulated and characterized in air. The photovoltaic performances were measured under the illumination of AM 1.5 G, 100 mW/cm^2 using a 300 W xenon solar simulator (Newport Oriel Solar Simulators). Current–voltage curves were measured using a Keithley 2420 source meter. The external quantum efficiency (EQE) was measured by Merlin lock-in amplifier coupled with CS260 monochromator and 300 W xenon lamp. The light intensity at each wavelength was calibrated with a standard single-crystal Si photovoltaic cell. The measurement of electron mobility was conducted in the dark by the space-charge limited current (SCLC) method on a computer-controlled Keithley 2420 source meter, for the electron-only devices. Electron-only devices with the structure ITO/Cs_2CO_3/blend/Ca/Al were fabricated by spin-coating the active layer on ITO/Cs_2CO_3 substrates followed by deposition of Ca/Al on the cathode electrode.

3. Results and discussion

3.1. Synthesis of $C_{60}(OCH_3)_4$ derivatives

Scheme 1 shows the two-step reaction for the synthesis of $C_{60}(OCH_3)_4$ derivatives starting from $C_{60}Cl_6$, which is a valuable substrate for preparation of novel fullerene derivatives by regio-selective substitution of chlorine atoms with appropriate organic groups [52–60]. Reacting with methanol in the presence of molecular oxygen in DMSO/chlorobenzene, in the present work, four of the six chlorine atoms in $C_{60}Cl_6$ were replaced to afford $C_{60}(OCH_3)_4$ as useful synthon ready for further functionalization. The 1,3-dipolar [3+2] cycloaddition of diazo or azide species to $C_{60}(OCH_3)_4$ has produced $C_{60}(OCH_3)_4$-PCBM or $C_{60}(OCH_3)_4$-APCBM with high regioselectivity. Both $C_{60}(OCH_3)_4$-PCBM and $C_{60}(OCH_3)_4$-APCBM, with good solubility in the common organic solvents such as chloroform, toluene, carbon disulfide, chlorobenzene, and o-dichlorobenzene, are readily purified by HPLC to give both of the multi-adduct fullerene electron acceptors in high purity.

The structures of both $C_{60}(OCH_3)_4$ derivatives were confirmed by ^1H and ^{13}C NMR spectra, and APCI mass spectra (see Figs. S1–S9). In contrast to $C_{60}(OCH_3)_4$-PCBM molecule, there is an additional nitrogen inset as bridge between the side chain and fullerene core in $C_{60}(OCH_3)_4$-APCBM. Such a trivial structure difference facilitates investigation of the influence of nitrogen bridge of PCBM-like fullerene derivative on photovoltaic performance.

3.2. Optical properties of $C_{60}(OCH_3)_4$ derivatives

Fig. 1 shows the UV–vis absorption spectra of $C_{60}(OCH_3)_4$-PCBM, $C_{60}(OCH_3)_4$-APCBM and PCBM in hexane solution with a concentration of 10^{-5} mol/L. In the visible region from 400 to 800 nm, the absorbance of $C_{60}(OCH_3)_4$-PCBM and $C_{60}(OCH_3)_4$-APCBM are almost the same, but in the UV region from 200 to 400 nm, the absorbance of $C_{60}(OCH_3)_4$-APCBM is slightly stronger
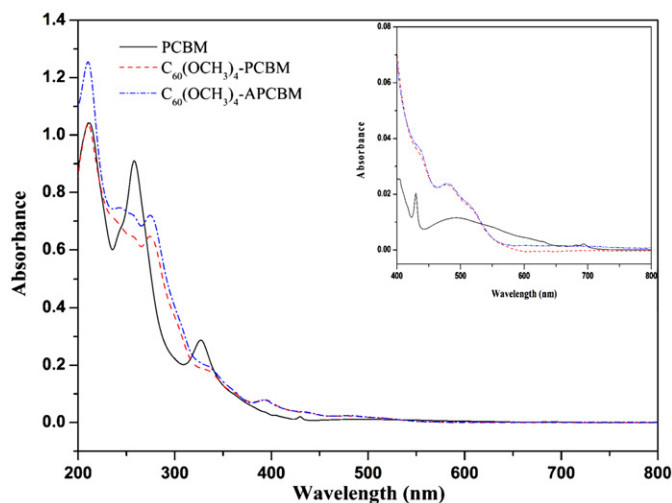
Fig. 1. UV–vis absorption spectra of $C_{60}(OCH_3)_4$-PCBM, $C_{60}(OCH_3)_4$-APCBM and PCBM in hexane solution (10^{-5} mol/L). Inset: enlarged absorption spectra in the visible region from 400 to 800 nm.
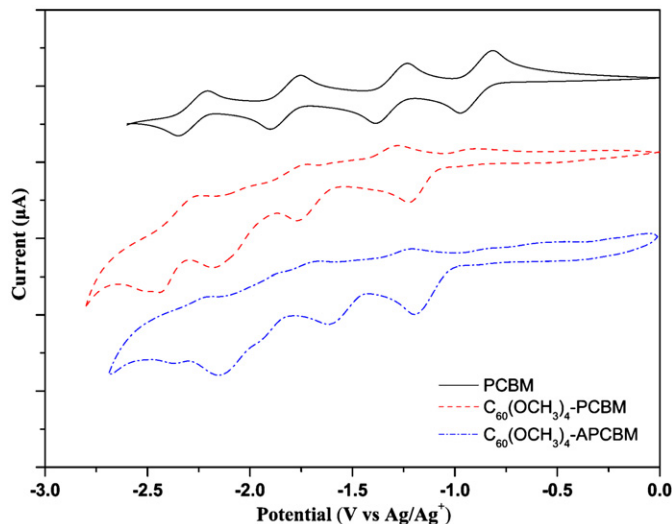

Fig. 2. Cyclic voltammograms of $C_{60}(OCH_3)_4$-PCBM, $C_{60}(OCH_3)_4$-APCBM and PCBM in a mixed solution of o-dichlorobenzene/acetonitrile (5:1) with 0.1 mol/L Bu_4NPF_6 at a scan rate of 100 mV/s.

than that of $C_{60}(OCH_3)_4$-PCBM. The absorbance of two $C_{60}(OCH_3)_4$ derivatives are much stronger than that of PCBM in the regions of 270–310 and 350–530 nm, which are expected beneficial to their application in PSCs. The optical bandgaps estimated from the absorption edges of $C_{60}(OCH_3)_4$-PCBM and $C_{60}(OCH_3)_4$-APCBM are 2.08 and 2.14 eV, respectively.

3.3. Electrochemical properties of $C_{60}(OCH_3)_4$ derivatives

The electrochemical properties of $C_{60}(OCH_3)_4$-PCBM, $C_{60}(OCH_3)_4$-APCBM and PCBM in the potential range of 0 to -2.8 V vs. Ag/Ag$^+$ were studied by cyclic voltammetry (Fig. 2). In the negative potential region, the reduction potentials of two $C_{60}(OCH_3)_4$ derivatives were negatively shifted with respect to PCBM. Four irreversible reduction waves were shown for each of the two $C_{60}(OCH_3)_4$ derivatives, in contrast to the reversible reduction waves of PCBM and APCBM [61,62]. The irreversible curves with bigger reduction peaks indicate that the $C_{60}(OCH_3)_4$ derivatives undergo decomposition, likely to lose methoxy, in the reduction process.

The LUMO energy level of fullerene derivative was estimated from its onset reduction potential according to the equation [63] LUMO$= -e(E_{red}^{on}+4.71)$ (eV), where E_{red}^{on} is the onset reduction potential in volt vs Ag/Ag$^+$. The onset reduction potentials (E_{red}^{on}) of PCBM, $C_{60}(OCH_3)_4$-PCBM and $C_{60}(OCH_3)_4$-APCBM are -0.80, -1.10 and -1.00 V vs Ag/Ag$^+$, respectively. Therefore, the calculated LUMO energy levels of $C_{60}(OCH_3)_4$-PCBM, $C_{60}(OCH_3)_4$-APCBM and PCBM are -3.61, -3.71 and -3.91 eV, respectively. The LUMO energy levels and the onset reduction potentials of the fullerene derivatives are listed in Table 1. The LUMO level of $C_{60}(OCH_3)_4$-PCBM and $C_{60}(OCH_3)_4$-APCBM are increased by 0.3 and 0.2 eV relative to that of PCBM, respectively. The higher LUMO energy level of $C_{60}(OCH_3)_4$ derivative relative to PCBM or APCBM, applicable in PSCs to increase open-circuit voltage, is almost certainly due to the multi-addition of electron donating methoxy groups on the fullerene core. On the other hand, it is demonstrated that the nitrogen bridge seems to slightly decrease the LUMO level, which is similar to the case of APCBM and PCBM previously reported in the literatures [61,62].

The HOMO levels of $C_{60}(OCH_3)_4$-PCBM and $C_{60}(OCH_3)_4$-APCBM were estimated to be -5.69 and -5.85 eV, respectively, according to the optical bandgaps obtained from the absorption spectrum, both higher than that of PCBM (-5.93 eV) [11]. For an acceptor, the higher HOMO level could lead to lower photochemical stability [64]. Therefore, the stability of the discussed fullerene derivatives is expected resulting in the order of PCBM $> C_{60}(OCH_3)_4$-APCBM $> C_{60}(OCH_3)_4$-PCBM.

3.4. Photovoltaic properties of $C_{60}(OCH_3)_4$ derivatives

For investigating the photovoltaic performances of $C_{60}(OCH_3)_4$ derivatives, PSCs were fabricated with P3HT as donor and $C_{60}(OCH_3)_4$ derivative as acceptor, and the weight ratio of the donor to the acceptor was 1:1. For comparison, P3HT/PCBM devices were also fabricated under otherwise identical conditions.

Fig. 3 shows the current density–voltage (J–V) curves of PSCs with P3HT as donor and $C_{60}(OCH_3)_4$ derivative or PCBM as acceptor, under the illumination of AM1.5G, 100 mW/cm^2. The data of open-circuit voltage, short-circuit current density (J_{sc}), fill factor (FF), and power conversion efficiency (PCE) of the devices are listed in Table 2. The V_{oc} of the device is increased from 0.58 V for PCBM to 0.63 V for $C_{60}(OCH_3)_4$-APCBM, and to 0.72 V for $C_{60}(OCH_3)_4$-PCBM. The higher V_{oc} values of the PSCs based on P3HT:$C_{60}(OCH_3)_4$ derivatives are obviously attributed to the higher LUMO energy levels of $C_{60}(OCH_3)_4$ derivatives relative to PCBM, because the V_{oc} of PSC is proportional to the difference between the HOMO energy level of the polymer donor and the LUMO energy level of the fullerene acceptor.

However, the relatively lower J_{sc} and FF of P3HT:$C_{60}(OCH_3)_4$ derivative device resulted in inefficient PCE. To clarify the mechanism responsible for the lower PCE, the electron mobility of P3HT:$C_{60}(OCH_3)_4$ derivatives in the bulk heterojunction active layer was evaluated by the space-charge limited current (SCLC) method. Fig. 4 shows the J–V curves of the electron-only devices (ITO/Cs$_2$CO$_3$/blend/Ca/Al) with P3HT blended with PCBM, $C_{60}(OCH_3)_4$-PCBM, or $C_{60}(OCH_3)_4$-APCBM. The electron mobilities of P3HT:PCBM, P3HT:$C_{60}(OCH_3)_4$-PCBM, and P3HT:$C_{60}(OCH_3)_4$-

Table 1
Onset reduction potentials, and LUMO energy levels of fullerene derivatives.

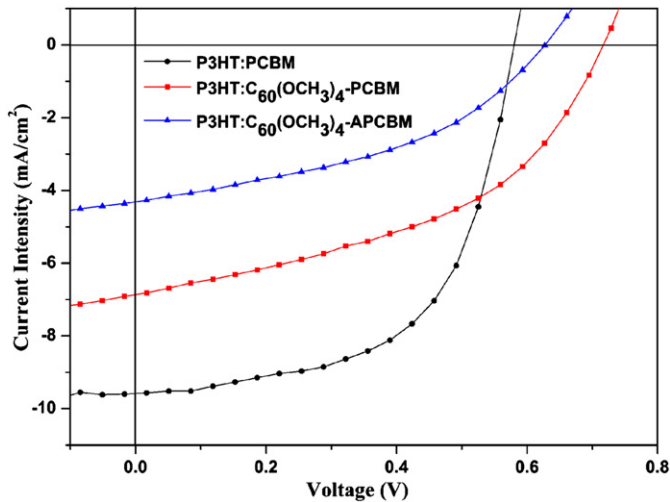| Compound	E_{red}^{on} (V)	LUMO (eV)
PCBM	-0.80	-3.91
$C_{60}(OCH_3)_4$-PCBM	-1.10	-3.61
$C_{60}(OCH_3)_4$-APCBM	-1.00	-3.71

Fig. 3. Current density–voltage (J–V) curves of PSCs with P3HT as donor and $C_{60}(OCH_3)_4$ derivative or PCBM as acceptor, under the illumination of AM1.5G, 100 mW/cm^2.

Table 2
Photovoltaic properties of devices with P3HT as donor and C_{60} derivative as acceptor.

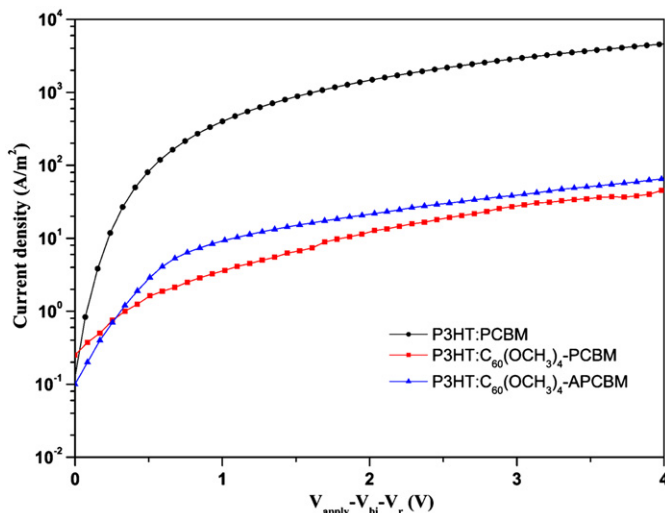| C_{60} derivative	V_{oc} (V)	J_{sc} (mA/cm^2)	FF (%)	PCE (%)
PCBM	0.58	9.56	58.7	3.25
$C_{60}(OCH_3)_4$-PCBM	0.72	6.86	45.3	2.24
$C_{60}(OCH_3)_4$-APCBM	0.63	4.30	42.2	1.14

Fig. 4. Measured space-charge limited J–V characteristics of the P3HT:PCBM/$C_{60}(OCH_3)_4$-PCBM/$C_{60}(OCH_3)_4$-APCBM blend devices under dark conditions for electron-only devices.

APCBM are 5.2×10^{-4}, 5.8×10^{-6}, and 6.5×10^{-6} cm^{2}V^{-1} s^{-1}, respectively. The electron mobility of $C_{60}(OCH_3)_4$ derivative ($C_{60}(OCH_3)_4$-PCBM or $C_{60}(OCH_3)_4$-APCBM) is approximately two orders of magnitude lower than that of PCBM, which is one of the reasons for the lower J_{sc} and FF in the P3HT:$C_{60}(OCH_3)_4$ derivative devices.

Specifically, the J_{sc} of P3HT:$C_{60}(OCH_3)_4$-APCBM device is fairly lower than that of $C_{60}(OCH_3)_4$-PCBM. Such a J_{sc} difference is almost certainly due to the structural difference of $C_{60}(OCH_3)_4$-APCBM from $C_{60}(OCH_3)_4$-PCBM, i.e., the nitrogen–carbon (N–C) bond bridging phenyl–butyric acid methyl ester (side chain) and

fullerene core. In principle, the single bond of N–C facilitates for rotation of the side chain against the fullerene core in $C_{60}(OCH_3)_4$-APCBM. As a result, disorder assembly of P3HT:$C_{60}(OCH_3)_4$-APCBM layer is highly possible because of the unavoidable conformational isomers of $C_{60}(OCH_3)_4$-APCBM resulting from the rotation of the side chain along with the axis of nitrogen bridge. Such a disorder assembly in P3HT:$C_{60}(OCH_3)_4$-APCBM active layer eventually leads to the lower J_{sc} in the photovoltaic device involved. The assumption about the possible rotation of the side chain along with the axis of N–C bond is supported by the clearly broad peaks in the ^{1}H NMR spectrum of $C_{60}(OCH_3)_4$-APCBM measured at room temperature (see Fig. S7a). Relatively narrow signals of ^{1}H NMR are shown in lower temperature ($-11.6°$ C) for the hydrogen atoms at the phenyl–butyric acid methyl ester group (see Fig. S7b), indicating the rotation of the side chain exists depending on temperature. To verify the rotation of the side chain along with the axis of N–C bond, we calculated the potential energy surface of $C_{60}(OCH_3)_4$-APCBM molecule with respect to the rotation of N–C bond using a combined quantum mechanics and molecular mechanics (QM/MM) approach. The NMR chemical shifts of $C_{60}(OCH_3)_4$-APCBM were also computed at the GIAO-B3LYP/6-31G** level of theory. The predicted ^{1}H and ^{13}C NMR chemical shifts agree with the experimental ones (see Supporting information for details).

External quantum efficiencies (EQEs) of PSCs with P3HT as donor and $C_{60}(OCH_3)_4$ derivative or PCBM as acceptor are shown in Fig. 5. The EQE value of P3HT:PCBM device is much higher than those of PSCs based on P3HT:$C_{60}(OCH_3)_4$ derivatives, which is consistent with the higher J_{sc} of P3HT:PCBM device.

3.5. Film morphologies

The film morphology of the photoactive layer influences the power conversion efficiency of PSCs to some extent [65,66]. AFM was used to investigate the morphology of blend films composed of P3HT and C_{60} derivative. The AFM topographic images of these blend films are shown in Fig. 6. The surface root mean square (rms) roughness is 1.6 nm for P3HT:PCBM film. As for P3HT:$C_{60}(OCH_3)_4$-PCBM and P3HT:$C_{60}(OCH_3)_4$-APCBM film, the rms is increased to 2.6 nm and 3.0 nm, respectively. The rougher surface morphology of P3HT:$C_{60}(OCH_3)_4$ derivative film may induce poorer contact between the active layer and the cathode, which partially accounts for the low FF of P3HT:$C_{60}(OCH_3)_4$ derivative device [66].
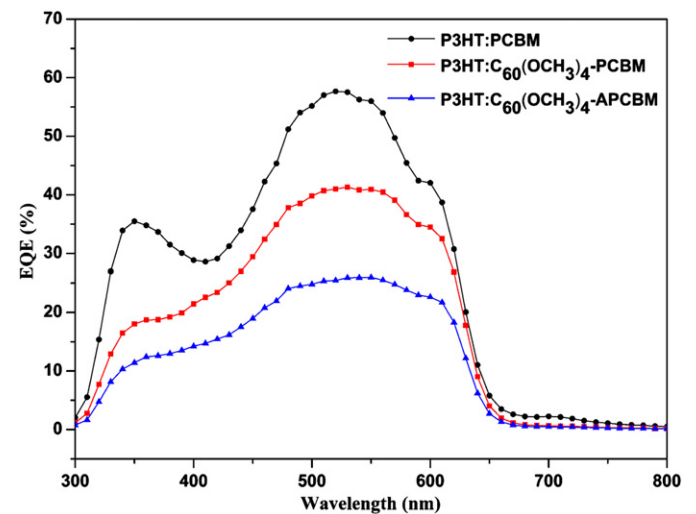

Fig. 5. External quantum efficiencies (EQEs) of PSCs with P3HT as donor and $C_{60}(OCH_3)_4$ derivative or PCBM as acceptor.
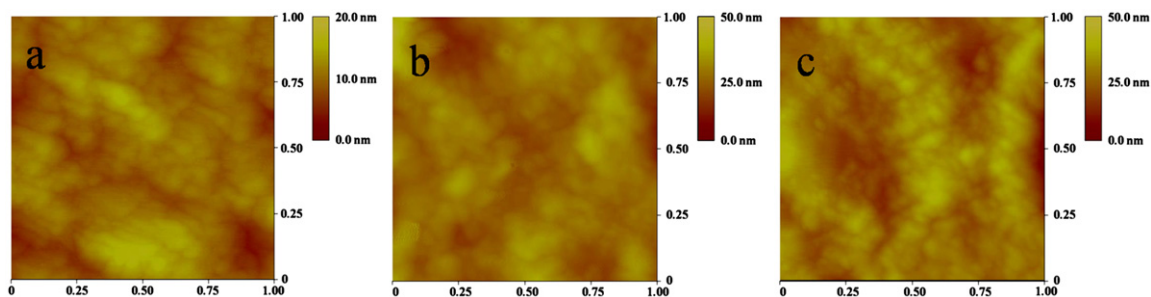
Fig. 6. AFM (1×1 μm^2) topography images of (a) P3HT:PCBM, (b) P3HT:$C_{60}(OCH_3)_4$-PCBM, and (c) P3HT:$C_{60}(OCH_3)_4$-APCBM.

4. Conclusions

We have synthesized two $C_{60}(OCH_3)_4$ derivatives, $C_{60}(OCH_3)_4$-PCBM and $C_{60}(OCH_3)_4$-APCBM by two-step reaction from $C_{60}Cl_6$ with high regioselectivity. The LUMO energy level of $C_{60}(OCH_3)_4$-PCBM (or $C_{60}(OCH_3)_4$-APCBM) is shown 0.3 eV (or 0.2 eV) higher than that of PCBM. Blended with P3HT, $C_{60}(OCH_3)_4$-PCBM and $C_{60}(OCH_3)_4$-APCBM photovoltaic devices show higher V_{oc} of 0.72 and 0.63 V, respectively. Likely due to low electron mobilities of the $C_{60}(OCH_3)_4$ derivatives, however, both J_{sc} and FF are poor for the devices based on $C_{60}(OCH_3)_4$-PCBM or $C_{60}(OCH_3)_4$-APCBM. The rotatable N–C single bond in $C_{60}(OCH_3)_4$-APCBM, as disclosed by the temperature-dependent NMR spectra and theoretical computations, restricts the photovoltaic performance such as J_{sc}. This work with two well-defined derivatives of fullerene as electron acceptors suggests that photovoltaic performances of PSC are susceptible to the structure of fullerene acceptor, and more fullerene derivatives are expected to be functionalized by multiple electron-donating groups for improving open-circuit voltage of PSC in the future.

Acknowledgments

Appendix A. Supporting information

Supplementary data associated with this article can be found in the online version at http://dx.doi.org/10.1016/j.solmat.2012.12.026.

References

[1] F.C. Krebs, Fabrication and processing of polymer solar cells: a review of printing and coating techniques, Solar Energy Materials and Solar Cells 93 (2009) 394–412.
[2] S. Gunes, H. Neugebauer, N.S. Sariciftci, Conjugated polymer-based organic solar cells, Chemical Reviews 107 (2007) 1324–1338.
[3] C.J. Brabec, N.S. Sariciftci, J.C. Hummelen, Plastic solar cells, Advanced Functional Materials 11 (2001) 15–26.
[4] F.C. Krebs, J. Fyenbo, M. Jorgensen, Product integration of compact roll-to-roll processed polymer solar cell modules: methods and manufacture using flexographic printing, slot-die coating and rotary screen printing, Journal of Materials Chemistry 20 (2010) 8994–9001.
[5] B.C. Thompson, J.M.J. Frechet, Polymer-fullerene composite solar cells, Angewandte Chemie, International Edition 47 (2008) 58–77.
[6] F.C. Krebs, T. Tromholt, M. Jorgensen, Upscaling of polymer solar cell fabrication using full roll-to-roll processing, Nanoscale 2 (2010) 873–886.
[7] F.C. Krebs, T.D. Nielsen, J. Fyenbo, M. Wadstrom, M.S. Pedersen, Manufacture, integration and demonstration of polymer solar cells in a lamp for the Lighting Africa initiative, Energy and Environmental Science 3 (2010) 512–525.
[8] S.C. Veenstra, W.J.H. Verhees, J.M. Kroon, M.M. Koetse, J. Sweelssen, J.J.A.M. Bastiaansen, H.F.M. Schoo, X. Yang, A. Alexeev, J. Loos, U.S. Schubert, M.M. Wienk, Photovoltaic properties of a conjugated polymer blend of MDMO-PPV and PCNEPV, Chemistry of Materials 16 (2004) 2503–2508.
[9] L. Schmidt-Mende, A. Fechtenkotter, K. Mullen, E. Moons, R.H. Friend, J.D. MacKenzie, Self-organized discotic liquid crystals for high-efficiency organic photovoltaics, Science 293 (2001) 1119–1122.
[10] F.G. Brunetti, X. Gong, M. Tong, A.J. Heeger, F. Wudl, Strain and huckel aromaticity: driving forces for a promising new generation of electron acceptors in organic electronics, Angewandte Chemie, International Edition 49 (2010) 532–536.
[11] Y.J. He, Y.F. Li, Fullerene derivative acceptors for high performance polymer solar cells, Physical Chemistry Chemical Physics 13 (2011) 1970–1983.
[12] C.J. Brabec, A. Cravino, D. Meissner, N.S. Sariciftci, T. Fromherz, M.T. Rispens, L. Sanchez, J.C. Hummelen, Origin of the open circuit voltage of plastic solar cells, Advanced Functional Materials 11 (2001) 374–380.
[13] C.J. Brabec, A. Cravino, D. Meissner, N.S. Sariciftci, M.T. Rispens, L. Sanchez, J.C. Hummelen, T. Fromherz, The influence of materials work function on the open circuit voltage of plastic solar cells, Thin Solid Films 403–404 (2002) 368–372.
[14] L.J.A. Koster, V.D. Mihailetchi, P.W.M. Blom, Ultimate efficiency of polymer/fullerene bulk heterojunction solar cells, Applied Physics Letters 88 (2006) 0935111–0935113.
[15] M.C. Scharber, D. Muehlbacher, M. Koppe, P. Denk, C. Waldauf, A.J. Heeger, C.J. Brabec, Design rules for donors in bulk-heterojunction solar cells-towards 10% energy-conversion efficiency, Advanced Materials 18 (2006) 789–794.
[16] F.B. Kooistra, J. Knol, F. Kastenberg, L.M. Popescu, W.J.H. Verhees, J.M. Kroon, J.C. Hummelen, Increasing the open circuit voltage of bulk-heterojunction solar cells by raising the LUMO level of the acceptor, Organic Letters 9 (2007) 551–554.
[17] N. Blouin, A. Michaud, D. Gendron, S. Wakim, E. Blair, R. Neagu-Plesu, M. Belletete, G. Durocher, Y. Tao, M. Leclerc, Toward a rational design of poly(2,7-Carbazole) derivatives for solar cells, Journal of the American Chemical Society 130 (2008) 732–742.
[18] E.G. Wang, L. Wang, L.F. Lan, C. Luo, W.L. Zhuang, J.B. Peng, Y. Cao, High-performance polymer heterojunction solar cells of a polysilafluorene derivative, Applied Physics Letters 92 (2008) 0333071–0333073.
[19] J.Y. Lee, S.W. Heo, H. Choi, Y.J. Kwon, J.R. Haw, D.K. Moon, Synthesis and characterization of 2,1,3-benzothiadiazole-thieno[3,2-b]thiophene-based charge transferred-type polymers for photovoltaic application, Solar Energy Materials and Solar Cells 93 (2009) 1932–1938.
[20] S.H. Park, A. Roy, S. Beaupre, S. Cho, N. Coates, J.S. Moon, D. Moses, M. Leclerc, K. Lee, A.J. Heeger, Bulk heterojunction solar cells with internal quantum efficiency approaching 100%, Nature Photonics 3 (2009) 297–303.
[21] R. Qin, W. Li, C. Li, C. Du, C. Veit, H.-F. Schleiermacher, M. Andersson, Z. Bo, Z. Liu, O. Inganas, U. Wuerfel, F. Zhang, A planar copolymer for high efficiency polymer solar cells, Journal of the American Chemical Society 131 (2009) 14612–14613.
[22] Y.Y. Liang, Z. Xu, J.B. Xia, S.-T. Tsai, Y. Wu, G. Li, C. Ray, L.P. Yu, For the bright future-bulk heterojunction polymer solar cells with power conversion efficiency of 7.4%, Advanced Materials 22 (2010) E135–E138.
[23] J.Y. Lee, S.H. Kim, I.S. Song, D.K. Moon, Efficient donor-acceptor type polymer semiconductors with well-balanced energy levels and enhanced open circuit voltage properties for use in organic photovoltaics, Journal of Materials Chemistry 21 (2011) 16480–16487.
[24] H.J. Song, D.H. Kim, E.J. Lee, S.W. Heo, J.Y. Lee, D.-K. Moon, Conjugated polymer consisting of quinacridone and benzothiadiazole as donor materials for organic photovoltaics: coplanar property of polymer backbone, Macro-molecules 45 (2012) 7815–7822.
[25] S.A. Backer, K. Sivula, D.F. Kavulak, J.M.J. Frechet, High efficiency organic photovoltaics incorporating a new family of soluble fullerene derivatives, Chemistry of Materials 19 (2007) 2927–2929.
[26] C. Yang, J.Y. Kim, S. Cho, J.K. Lee, A.J. Heeger, F. Wudl, Functionalized methanofullerenes used as n-type materials in bulk-heterojunction polymer

solar cells and in field-effect transistors, Journal of the American Chemical Society 130 (2008) 6444–6450.

[27] Y. Zhang, H.-L. Yip, O. Acton, S.K. Hau, F. Huang, A.K.Y. Jen, A simple and effective way of achieving highly efficient and thermally stable bulk-heterojunction polymer solar cells using amorphous fullerene derivatives as electron acceptor, Chemistry of Materials 21 (2009) 2598–2600.

[28] A. Varotto, N.D. Treat, J. Jo, C.G. Shuttle, N.A. Batara, F.G. Brunetti, J.H. Seo, M.L. Chabinyc, C.J. Hawker, A.J. Heeger, F. Wudl, 1,4-Fullerene derivatives: tuning the properties of the electron transporting layer in bulk-heterojunction solar cells, Angewandte Chemie, International Edition 50 (2011) 5166–5169.

[29] M. Lenes, G.-J.A.H. Wetzelaer, F.B. Kooistra, S.C. Veenstra, J.C. Hummelen, P.W.M. Blom, Fullerene bisadducts for enhanced open-circuit voltages and efficiencies in polymer solar cells, Advanced Materials 20 (2008) 2116–2119.

[30] M. Lenes, S.W. Shelton, A.B. Sieval, D.F. Kronholm, J.C. Hummelen, P.W.M. Blom, Electron trapping in higher adduct fullerene-based solar cells, Advanced Functional Materials 19 (2009) 3002–3007.

[31] J.H. Choi, K.-I. Son, T. Kim, K. Kim, K. Ohkubo, S. Fukuzumi, Thienyl-substituted methanofullerene derivatives for organic photovoltaic cells, Journal of Materials Chemistry 20 (2010) 475–482.

[32] Y.J. He, H.-Y. Chen, J.H. Hou, Y.F. Li, Indene-C_{60} bisadduct: a new acceptor for high-performance polymer solar cells, Journal of the American Chemical Society 132 (2010) 1377–1382.

[33] Y.J. He, G.J. Zhao, B. Peng, Y.F. Li, High-yield synthesis and electrochemical and photovoltaic properties of indene-C_{70} bisadduct, Advanced Functional Materials 20 (2010) 3383–3389.

[34] Y. Zhang, Y. Matsuo, C.-Z. Li, H. Tanaka, E. Nakamura, A scalable synthesis of methano[60]fullerene and congeners by the oxidative cyclopropanation reaction of silylmethylfullerene, Journal of the American Chemical Society 133 (2011) 8086–8089.

[35] C.-Z. Li, S.-C. Chien, H.-L. Yip, C.-C. Chueh, F.-C. Chen, Y. Matsuo, E. Nakamura, A.K.Y. Jen, Facile synthesis of a 56pi-electron 1,2-dihydromethano-[60]PCBM and its application for thermally stable polymer solar cells, Chemical Communications 47 (2011) 10082–10084.

[36] Y.J. He, B. Peng, G.J. Zhao, Y.P. Zou, Y.F. Li, Indene addition of [6,6]-phenyl-C_{61}-butyric acid methyl ester for high-performance acceptor in polymer solar cells, Journal of Physical Chemistry C 115 (2011) 4340–4344.

[37] J.A. Mikroyannidis, D.V. Tsagkournos, S.S. Sharma, G.D. Sharma, Synthesis of a broadly absorbing modified PCBM and application as electron acceptor with poly(3-hexylthiophene) as electron donor in efficient bulk heterojunction solar cells, Journal of Physical Chemistry C 115 (2011) 7806–7816.

[38] Y.J. He, H.-Y. Chen, G.J. Zhao, J.H. Hou, Y.F. Li, Biindene-C_{60} adducts for the application as acceptor in polymer solar cells with higher open-circuit-voltage, Solar Energy Materials and Solar Cells 95 (2011) 899–903.

[39] C.-L. Chang, C.-W. Liang, J.-J. Syu, L.-J. Wang, M.-K. Leung, Triphenylamine-substituted methanofullerene derivatives for enhanced open-circuit voltages and efficiencies in polymer solar cells, Solar Energy Materials and Solar Cells 95 (2011) 2371–2379.

[40] Y.-J. Cheng, M.-H. Liao, C.-Y. Chang, W.-S. Kao, C.-E. Wu, C.-S. Hsu, Di(4-methylphenyl)methano-C_{60} bis-adduct for efficient and stable organic photovoltaics with enhanced open-circuit voltage, Chemistry of Materials 23 (2011) 4056–4062.

[41] K.-H. Kim, H. Kang, S.Y. Nam, J. Jung, P.S. Kim, C.-H. Cho, C.J. Lee, S.C. Yoon, B.J. Kim, Facile synthesis of o-xylenyl fullerene multiadducts for high open circuit voltage and efficient polymer solar cells, Chemistry of Materials 23 (2011) 5090–5095.

[42] E. Voroshazi, K. Vasseur, T. Aernouts, P. Heremans, A. Baumann, C. Deibel, X. Xue, A.J. Herring, A.J. Athans, T.A. Lada, H. Richter, B.P. Rand, Novel bis-C_{60} derivative compared to other fullerene bis-adducts in high efficiency polymer photovoltaic cells, Journal of Materials Chemistry 21 (2011) 17345–17352.

[43] X.Y. Meng, W.Q. Zhang, Z.-a. Tan, C. Du, C.H. Li, Z.S. Bo, Y.F. Li, X.L. Yang, M.M. Zhen, F. Jiang, J.P. Zheng, T.S. Wang, L. Jiang, C.Y. Shu, C.R. Wang, Dihydronaphthyl-based [60]fullerene bisadducts for efficient and stable polymer solar cells, Chemical Communications 48 (2012) 425–427.

[44] X.Y. Meng, W.Q. Zhang, Z.a. Tan, Y.F. Li, Y.H. Ma, T.S. Wang, L. Jiang, C.Y. Shu, C.R. Wang, Highly efficient and thermally stable polymer solar cells with dihydronaphthyl-based [70]fullerene bisadduct derivative as the acceptor, Advanced Functional Materials 22 (2012) 2187–2193.

[45] C.Y. Zhang, S. Chen, Z. Xiao, Q.Q. Zuo, L.M. Ding, Synthesis of mono- and bisadducts of thieno-o-quinodimethane with C_{60} for efficient polymer solar cells, Organic Letters 14 (2012) 1508–1511.

[46] L.-L. Deng, J. Feng, L.-C Sun, S. Wang, S.-L. Xie, S.-Y. Xie, R.-B. Huang, L.-S. Zheng, Functionalized dihydronaphthyl-C_{60} derivatives as acceptors for efficient polymer solar cells with tunable photovoltaic properties, Solar Energy Materials and Solar Cells 104 (2012) 113–120.

[47] K.-H. Kim, H. Kang, H.J. Kim, P.S. Kim, S.C. Yoon, B.J. Kim, Effects of solubilizing group modification in fullerene bis-adducts on normal and inverted type polymer solar cells, Chemistry of Materials 24 (2012) 2373–2381.

[48] J.M. Frost, M.A. Faist, J. Nelson, Energetic disorder in higher fullerene adducts: a quantum chemical and voltammetric study, Advanced Materials 22 (2010) 4881–4884.

[49] N.C. Miller, S. Sweetnam, E.T. Hoke, R. Gysel, C.E. Miller, J.A. Bartelt, X.X. Xie, M.F. Toney, M.D. McGehee, Molecular packing and solar cell performance in blends of polymers with a bisadduct fullerene, Nano Letters 12 (2012) 1566–1570.

[50] R.K.M. Bouwer, G.-J.A.H. Wetzelaer, P.W.M. Blom, J.C. Hummelen, Influence of the isomeric composition of the acceptor on the performance of organic bulk heterojunction P3HT:bis-PCBM solar cells, Journal of Materials Chemistry 22 (2012) 15412–15417.

[51] P.R. Birkett, A.G. Avent, A.D. Darwish, H.W. Kroto, R. Taylor, D.R.M. Walton, Preparation and ^{13}C NMR spectroscopic characterisation of $C_{60}Cl_6$, Journal of the Chemical Society, Chemical Communications (1993) 1230–1232.

[52] P.R. Birkett, A.G. Avent, A.D. Darwish, H.W. Kroto, R. Taylor, D.R.M. Walton, Preparation and characterization of unsymmetrical C60Ph4 and symmetrical $C_{60}Ph_2$: the effect of regioselective nucleophilic attack upon $C_{60}Cl_6$, Journal of the Chemical Society, Perkin Transactions 2 (1997) 457–461.

[53] A.a.K. Abdul-Sada, A.G. Avent, P.R. Birkett, H.W. Kroto, R. Taylor, D.R.M. Walton, A hexaallyl[60]fullerene, $C_{60}(CH_2CH:CH_2)_6$, Journal of the Chemical Society, Perkin Transactions 1: Organic and Bio-Organic Chemistry (1998) 393–396.

[54] H. Al-Matar, P.B. Hitchcock, A.G. Avent, R. Taylor, Isolation and characterization of Cs-symmetry $C_{60}Me_5O_2OH$, the first methylated fullerenol; a bis-epoxide with two oxygens in a pentagonal ring, Chemical Communications (2000) 1071–1072.

[55] A.G. Avent, P.R. Birkett, A.D. Darwish, S. Houlton, R. Taylor, K.S.T. Thomson, X.-W. Wei, Formation and characterization of alkoxy derivatives of [60]fullerene, Journal of the Chemical Society, Perkin Transactions 2 (2001) 782–786.

[56] H. Al-Matar, A.a.K. Abdul-Sada, A.G. Avent, P.W. Fowler, P.B. Hitchcock, K.M. Rogers, R. Taylor, Isolation and characterization of symmetrical $C_{60}Me_6$, $C_{60}Me_5Cl$ and $C_{60}Me_5O_2OH$, together with unsymmetrical $C_{60}Me_5O_3H$, $C_{60}Me_5OOH$, $C_{60}Me_4PhO_2OH$, and $C_{60}Me_{12}$; fragmentation of methylfullerenols to C_{58}, Journal of the Chemical Society, Perkin Transactions 2 (2002) 53–58.

[57] O.A. Troshina, P.A. Troshin, A.S. Peregudov, E.M. Balabaeva, V.I. Kozlovski, R.N. Lyubovskaya, Reactions of chlorofullerene $C_{60}Cl_6$ with N-substituted piperazines, Tetrahedron 62 (2006) 10147–10151.

[58] P.A. Troshin, E.A. Khakina, A.S. Peregudov, D.V. Konarev, I.V. Soulimenkov, S.M. Peregudova, R.N. Lyubovskaya, $[C_{60}(CN)5]^-$: a remarkably stable [60]fullerene anion, European Journal of Organic Chemistry 2010 (2010) 3265–3268.

[59] A.B. Kornev, E.A. Khakina, S.I. Troyanov, A.A. Kushch, A. Peregudov, A. Vasilchenko, D.G. Deryabin, V.M. Martynenko, P.A. Troshin, Facile preparation of amine and amino acid adducts of [60]fullerene using chlorofullerene $C_{60}Cl_6$ as a precursor, Chemical Communications 48 (2012) 5461–5463.

[60] E.A. Khakina, A.A. Yurkova, A.S. Peregudov, S.I. Troyanov, V.V. Trush, A.I. Vovk, A.V. Mumyatov, V.M. Martynenko, J. Balzarini, P.A. Troshin, Highly selective reactions of $C_{60}Cl_6$ with thiols for the synthesis of functionalized [60]fullerene derivatives, Chemical Communications 48 (2012) 7158–7160.

[61] S.H. Park, C. Yang, S. Cowan, J.K. Lee, F. Wudl, K. Lee, A.J. Heeger, Isomeric iminofullerenes as acceptors in bulk heterojunction organic solar cells, Journal of Materials Chemistry 19 (2009) 5624–5628.

[62] C. Yang, S. Cho, A.J. Heeger, F. Wudl, Heteroanalogues of PCBM: n-bridged imino-PCBMs for organic field-effect transistors, Angewandte Chemie, International Edition 48 (2009) 1592–1595.

[63] Q.J. Sun, H.Q. Wang, C.H. Yang, Y.F. Li, Synthesis and electroluminescence of novel copolymers containing crown ether spacers, Journal of Materials Chemistry 13 (2003) 800–806.

[64] T. Tromholt, M.V. Madsen, J.E. Carle, M. Helgesen, F.C. Krebs, Photochemical stability of conjugated polymers, electron acceptors and blends for polymer solar cells resolved in terms of film thickness and absorbance, Journal of Materials Chemistry 22 (2012) 7592–7601.

[65] W.L. Ma, C.Y. Yang, X. Gong, K. Lee, A.J. Heeger, Thermally stable efficient polymer solar cells with nanoscale control of the interpenetrating network morphology, Advanced Functional Materials 15 (2005) 1617–1622.

[66] G. Li, V. Shrotriya, J.S. Huang, Y. Yao, T. Moriarty, K. Emery, Y. Yang, High-efficiency solution processable polymer photovoltaic cells by self-organization of polymer blends, Nature Materials 4 (2005) 864–868.